Article

Determination of Global Structure from Distance and Orientation Constraints in Biological Solids Using Solid-State NMR Spectroscopy

Loren B. Andreas, Anil K. Mehta, and Manish A. Mehta

J. Am. Chem. Soc., **2007**, 129 (49), 15233-15239 • DOI: 10.1021/ja074789q

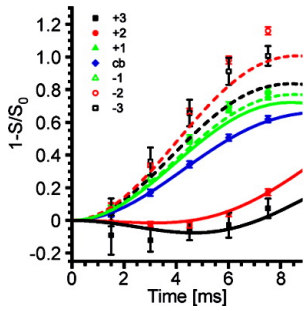

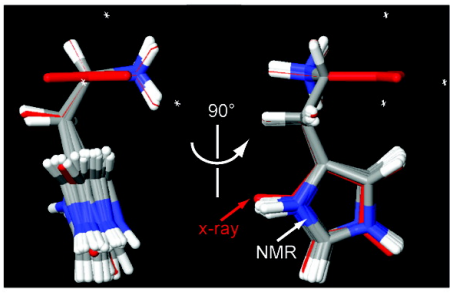

More About This Article

Additional resources and features associated with this article are available within the HTML version:

- Supporting Information
- Access to high resolution figures
- Links to articles and content related to this article
- Copyright permission to reproduce figures and/or text from this article

View the Full Text HTML

J|A|C|S
ARTICLES
Published on Web 11/09/2007

Determination of Global Structure from Distance and Orientation Constraints in Biological Solids Using Solid-State NMR Spectroscopy

Loren B. Andreas,[†] Anil K. Mehta,*[,‡] and Manish A. Mehta*[,†]

Contribution from the Department of Chemistry and Biochemistry, Oberlin College, Oberlin, Ohio 44074, and Department of Chemistry, Emory University, Atlanta, Georgia 30322

Received June 29, 2007; E-mail: anil.mehta@emory.edu; manish.mehta@oberlin.edu

Abstract: We report the results from a new solid-state NMR experiment, DANTE−REDOR, which can determine global secondary structure in uniformly (^{13}C,^{15}N)-enriched systems by simultaneously measuring distance and orientation constraints. Following a heteronuclear spin-pair selection using a DANTE pulse train, the magnitude and orientation of the internuclear dipole vector, within the chemical shift anisotropy (CSA) frame of the observed nucleus, are determined by tracking the dephasing of individual spinning sidebands under magic angle spinning. The efficacy of the experiment is demonstrated by measuring the imidazole side-chain orientation in U-[$^{13}C_6$,$^{15}N_3$]-L-histidine·HCl·H_2O.

Introduction

A recently developed class of dipolar recoupling NMR experiments has enabled structural interrogation of proteins in the solid state[1−6] and are now beginning to realize their full potential for elucidating global backbone and side-chain structure in large, uniformly labeled proteins. These approaches determine a series of internuclear distances by selectively reintroducing dipolar couplings,[3,5] yet they fail to exploit the panoply of information embedded within anisotropic interactions, such as chemical shift anisotropy (CSA).[7,8] We report here a new solid-state NMR experiment, DANTE−REDOR (Figure 1) that has the capacity to yield global structure in uniformly labeled peptides and proteins. Our procedure extracts both molecular orientation information encoded in magic-angle spinning (MAS) sidebands and internuclear distances of chemical-shift resolved resonances and can, for example, constrain amino acid side-chain atom positions in relation to the backbone. This experiment brings together the specificity and accuracy enjoyed by techniques that rely on site-specific isotopic labels with the synthetic convenience of a single, uniformly labeled sample under non-exotic experimental conditions. We demonstrate the efficacy of the experiment by determining the imidazole side-chain orientation with respect to the backbone in U-[$^{13}C_6$,$^{15}N_3$]-L-histidine·HCl·H_2O.

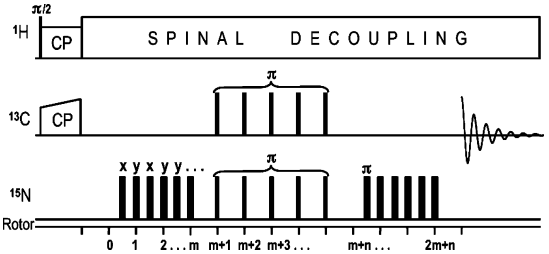

Figure 1. Pulse scheme for the $^{13}C\{^{15}N\}$DANTE−REDOR experiment. The rotor-synchronized pulses in the middle of the sequence on both the ^{13}C and ^{15}N channels represent the collective π-DANTE pulse. ^{15}N REDOR π-pulses follow the *xy*-8 phase cycling scheme.

In pairwise labeled samples the rotational-echo double-resonance (REDOR) experiment can extract distances between heteronuclei, such as ^{13}C and ^{15}N.[9,10] It has been shown that the orientation of the internuclear dipolar vector, with respect to the CSA frame of the observed spin, is also encoded in REDOR dephasing of spinning sidebands.[11,12] In uniformly labeled solids, the measurement of $^{13}C-^{15}N$ distances with the REDOR experiment is compromised by both homonuclear $^{13}C-^{13}C$ *J* couplings and multiple $^{13}C-^{15}N$ dipolar couplings.[13] In this case, the RDX sequence (REDOR of $^{13}C_x$) can be used to simultaneously measure multiple $^{13}C-^{15}N$ distances when only a single ^{15}N is present; however, this does require that exact simulations for each spin-system and conformation be performed[5,13] which precludes the use of the analytical expression derived for REDOR dephasing.[12,14] In the case where the chemical shifts of ^{13}C and ^{15}N resonances are resolved,

[†] Oberlin College.
[‡] Emory University.

(1) Michal, C. A.; Jelinski, L. W. *J. Am. Chem. Soc.* **1997**, *119*, 9059−9060.
(2) Jaroniec, C. P.; Tounge, B. A.; Rienstra, C. M.; Herzfeld, J.; Griffin, R. G. *J. Am. Chem. Soc.* **1999**, *121*, 10237−10238.
(3) Jaroniec, C. P.; Tounge, B. A.; Herzfeld, J.; Griffin, R. G. *J. Am. Chem. Soc.* **2001**, *123*, 3507−3519.
(4) Castellani, F.; van Rossum, B.; Diehl, A.; Schubert, M.; Rehbein, K.; Oschkinat, H. *Nature* **2002**, *420*, 98−102.
(5) Mehta, A. K.; Cegelski, L.; O'Connor, R. D.; Schaefer, J. *J. Magn. Reson.* **2003**, *163*, 182−187.
(6) Ladizhansky, V.; Griffin, R. G. *J. Am. Chem. Soc.* **2004**, *126*, 948−958.
(7) Stoll, M. E.; Vega, A. J.; Vaughan, R. W. *J. Chem. Phys.* **1976**, *65*, 4093−4098.
(8) Munowitz, M. G.; Griffin, R. G.; Bodenhausen, G.; Huang, T. H. *J. Am. Chem. Soc.* **1981**, *103*, 2529−2533.
(9) Gullion, T.; Schaefer, J. *J. Magn. Reson.* **1989**, *81*, 196−200.
(10) Gullion, T.; Schaefer, J. *Adv. Magn. Reson.* **1989**, *13*, 58−83.
(11) Goetz, J. M.; Schaefer, J. *J. Magn. Reson.* **1997**, *129*, 222−223.
(12) O'Connor, R. D.; Schaefer, J. *J. Magn. Reson.* **2002**, *154*, 46−52.
(13) Mehta, A. K.; Schaefer, J. *J. Magn. Reson.* **2003**, *163*, 188−191.

frequency-selective REDOR (FS-REDOR) has been used to measure specific $^{13}C-^{15}N$ heteronuclear distances,[2,3] but because of the use of fast magic angle spinning and shaped selective pulses, spinning sidebands and precious orientation information therein are eliminated. The core of our approach is to extend the frequency-selective REDOR sequence by using a DANTE (delays alternating with nutation for tailored excitation) spin selection method,[15] to select a specific resonance and its attendant sidebands.[16] When combined with the REDOR experiment, both the heteronuclear distance and the dipole-CSA orientation can be extracted for a specific spin pair in a uniformly labeled system using the exact same equations[12,14] for the isolated pairwise labeled spin system. We show below that measuring multiple heteronuclear distances and dipole-CSA orientations within the same sample is sufficient to converge on a global structure.

Experimental Methods

Sample Preparation and Characterization. Polycrystalline U-[$^{13}C_6$,$^{15}N_3$]-L-histidine·HCl·H_2O was produced by dissolving 1 molar part neat U-[$^{13}C_6$,$^{15}N_3$]-L-histidine·HCl·H_2O (Cambridge Isotope Labs, Cambridge, MA) and 9 molar parts natural abundance L-histidine·HCl·H_2O (Sigma Aldrich, St. Louis, MO) in water, and slowly recrystallizing the aqueous solution at room temperature. Dilution percentage was determined to be 10.0% by an electrospray mass spectral analysis (Combinix, CA). A second sample was recrystallized at 5% dilution to check for intermolecular multispin effects by dissolving 1 molar part neat U-[$^{13}C_6$,$^{15}N_3$]-L-histidine·HCl·H_2O and 19 molar parts natural abundance L-histidine·HCl·H_2O.

X-ray Diffraction. The full crystal structure of a representative crystal from the 10% dilution crystallization batch was determined at the Youngstown State University crystallography center. The structure and complete refinement data are given in the Supporting Information. The structure has been deposited into the Cambridge Crystallographic Structural Database (CCDC 651941).[17]

Powder diffraction measurements were made using a Philips MPD-3040 X-ray powder diffractometer, with a copper-α source (wavelength 1.54 Å). Powder diffraction traces (see Supporting Information, Figure S1) were collected using a continuous scan from 4.5° to 50.5° in 2θ incrementing at a rate of 0.0125 degrees/sec. Counts were recorded every 0.05°4″, with each scan taking approximately 50 min. Software packages CrystalMaker and CrystalDiffract were used to compare the collected powder pattern with that predicted from the experimentally determined crystal structure to confirm that all NMR samples were of the same polymorph. Such checks were performed for each sample used in the NMR experiments.

NMR Spectroscopy. All spectra were collected on a custom-assembled system at Oberlin College consisting of a 14.1 T, 54 mm bore magnet (600.381 MHz for ^1H; 150.987 MHz for ^{13}C; 60.84 MHz for ^{15}N; Magnex Scientific; Oxford, England), a 39-channel room-temperature shim system (Resonance Research Inc.; Billerica, MA), a three-channel console (TecMag Inc.; Houston, TX), and a triple-resonance 4 mm magic angle spinning probe (Doty Scientific Inc.; Columbia, SC). The spinning frequency of 5319 Hz was carefully chosen to avoid a multitude of rotational resonance conditions (see below) and regulated to ± 2 Hz using a custom-built spin controller. The sample was restricted to the center third of the rotor, which resulted in RF inhomogeneity of ~2 to 5% fwhm as measured using the nutation method.[18] The damping factor was ~3 rad/ms and the nutation frequency was ~31 kHz. It has been our experience that sample restriction is not necessary for the REDOR experiment. Although not tested, RF inhomogeneity may affect the ability of the DANTE pulse to refocus the homonuclear *J* couplings, which could complicate the REDOR analysis. However, the varying of the amplitude of the DANTE pulses[16] or high homogeneity RF coils may prevent any deleterious effects on DANTE selection.

DANTE−REDOR Experimental Details. DANTE pulses were calibrated using the pulse sequence: $CP_x-(\pi/2)_y-$DANTE$-\pi/2-$acquire. DANTE pulse lengths and durations were fixed and the amplitude was adjusted for maximum signal intensity. A loss in signal proportional to T_2 relaxation corresponding to the total length of the DANTE pulse train was observed. The selective DANTE refocusing pulses were phase cycled 0123, while the receiver was cycled 0202, which cancels signal not affected by the selective pulse and compensates for an imperfect π-pulse. The initial proton $\pi/2$ pulse phase was cycled 1313.

The $^{13}C\{^{15}N\}$DANTE−REDOR pulse sequence was adapted from the FS-REDOR pulse sequence[3] using DANTE selective pulses as depicted in Figure 1. Following $^1H-^{13}C$ cross-polarization via a linearly ramped ^{13}C CP pulse, $^{13}C-^{15}N$ dipolar couplings are reintroduced using the $^{13}C\{^{15}N\}$REDOR sequence.[9] Rotor-synchronized ^{15}N 16 μs π-pulses separated by half a rotor-period ($\tau_r/2$) were *xy*-8 phase cycled.[19] All REDOR dephasing pulses were placed on the ^{15}N channel to avoid homonuclear recoupling of ^{13}C nuclei. Rotor-synchronized frequency selective DANTE π pulses were applied on both the ^{13}C and ^{15}N channels. This inverts specific ^{13}C and ^{15}N resonances and all intensities spaced by the spinning frequency, including the spinning sidebands. Care must be taken to avoid accidental inversion of peaks separated by integer multiples of the rotor frequency; however, this is already a constraint in uniformly labeled systems where it is important to avoid rotational resonance conditions. The selective pulses ensure that in the second symmetrically placed REDOR evolution period all heteronuclear $^{13}C-^{15}N$ dipolar couplings are refocused except between the selected $^{13}C-^{15}N$ spin pair. The ^{15}N dephasing pulses after the selective DANTE pulses are shifted by $\tau_r/2$ with respect to their position in the traditional single-pulse REDOR experiment.[9] In addition, the selective ^{13}C π-pulse refocuses all $^{13}C-^{13}C$ *J*-couplings to the selected ^{13}C. The selective ^{13}C π pulse is phase-cycled to remove all signals that are unaffected by this pulse. Thus, at the end of the REDOR evolution time, the ^{13}C spin−echo intensity is modulated only by dipolar couplings to the selected ^{15}N. The resulting REDOR curve can be fit to the analytical expression for an isolated spin-pair.[12,14] The REDOR dephasing time is $2m\tau_r$ (Figure 1). The number of REDOR rotor cycles (m) applied symmetrically before and after the selective pulse was incremented in multiples of 4 to implement *xy*-8 phase cycling.[19] Phase of the initial proton $\pi/2$ pulse was cycled as 11113333, phase of the observed spin DANTE pulse (^{13}C) was cycled as 0123, and the receiver phase was cycled as 02022020 to compensate for background ^{13}C signal, remove resonances not affected by the selective pulses, and compensate for ^{13}C π-pulse imperfections. Unless otherwise indicated, the proton decoupling field was 100 kHz (SPINAL-64)[20] and the DANTE π-pulse trains consisted of 33 2 μs rotor-synchronized pulses. Fourier transforms were applied with no apodization and zero filling to twice the acquisition time of 15.36 ms. Only zero-order phase correction was used. S and S_0 intensities were determined by measuring spectral peak heights.

MAS Spectra, Carbonyl Carbon CSA Tensor Principal Values and Assignment. X-ray powder diffraction patterns were collected for all NMR samples to confirm all samples were the same polymorph. The ^{13}C and ^{15}N CP/MAS spectra are shown in the Supporting

(14) Mueller, K. T.; Jarvie, T. P.; Aurentz, D. J.; Roberts, B. W. *Chem. Phys. Lett.* **1995**, *242*, 535−542.
(15) Morris, G. A.; Freeman, R. *J. Magn. Reson.* **1978**, *29*, 433−462.
(16) Theimer, D.; Bodenhausen, G. *Appl. Magn. Reson.* **1992**, *3*, 981−998.
(17) Zeller, M.; Bhate, M. P.; Mehta, M. A. *CCDC 651941*; Cambridge Crystallographic Data Centre (CCDC): Cambridge, U.K. 2007.
(18) Martin, M. L.; Delpuech, J. J.; Martin, G. J. *Practical NMR Spectroscopy*; Heyden: London, 1980.
(19) Gullion, T.; Baker, D. B.; Conradi, M. S. *J. Magn. Reson.* **1990**, *89*, 479−484.
(20) Fung, B. M.; Khitrin, A. K.; Ermolaev, K. *J. Magn. Reson.* **2000**, *142*, 97−101.

Information (Figure S2). Intensities of the spinning sidebands from the ^{13}C CP/MAS spectrum were used in a Herzfeld−Berger[21] analysis with the WinSolids HBA[22] program to determine the principal components of the carbonyl carbon ($^{13}C'$) shift tensor.

Carbon connectivity, hence assignment, was determined via the two-dimensional homonuclear correlation experiment, SPC-5.[23] Experimental details and the 2D correlation spectrum are given in the Supporting Information (Figures S3 and S4). ^{15}N resonances were assigned using $^{13}C\{^{15}N\}$DANTE−REDOR to measure the dipolar couplings between the non-protontated imidazole ring $^{13}C_\gamma$ and the two ring nitrogens of ~900 and 200 Hz for N_δ and N_ϵ, respectively.

Rotational Resonance (R^2) Conditions. Rotational resonance[24] conditions abound in uniformly labeled samples. The R^2 map of all first-order rotational resonance conditions in U-[$^{13}C_6$,$^{15}N_3$]-L-histidine·HCl·H_2O is shown in Figure S5. The rotational resonance conditions were computed by selecting all spin pairs (i,j) less than 5 Å apart in the crystal structure and solving for the spinning speed ν_r in the expression $\nu_i - \nu_j = n\nu_r$, where ν_i and ν_j are the isotropic chemical shifts of the spins in Hertz and n is held at 1. Since each rotational resonance condition has a finite width, experiments in this work were performed at least 200 Hz from any R^2 condition.

NMR Data Analysis and Simulation. Internuclear distances were determined by fitting the experimental $^{13}C\{^{15}N\}$DANTE−REDOR data points to the analytical expression for the REDOR dephasing,[14]

$$\Delta S/S_0(\tau) = \lambda[1 - \langle\cos(\omega_{CN}\tau)\rangle]$$

using Mathematica or MATLAB. $\Delta S/S_0 = 1 - S/S_0$, where S and S_0 are the REDOR dephased and full-echo intensities, respectively. The coupling ω_{CN} is a function of the dipolar coupling constant, $b_{CN} = -\mu_0\gamma_C\gamma_N\hbar/4\pi r_{CN}^3$ where r_{CN} is the internuclear ^{13}C-^{15}N distance, and $\langle\,\rangle$ indicates the powder average over a uniform distribution of crystallite orientations. The scaling factor λ accounts for ^{13}C spins without a neighboring ^{15}N spin, which is a result of 99% isotopic enrichment, dilution of the labeled compound in natural abundance material, imperfect ^{13}C and ^{15}N inversions pulses, and decay of coherence due to insufficient decoupling.

For the distance measurement,

$$\chi_\nu^2 \propto \sqrt{\sum_i \left(\left(\left(\frac{\Delta S}{S_0}\right)_{i,\,\mathrm{exp}} - \left(\frac{\Delta S}{S_0}\right)_{i,\mathrm{sim}}\right)/\left(\frac{\Delta S}{S_0}\right)_{i,\,\mathrm{exp}}\right)^2}$$

was minimized to fit the data, where the sum over i is taken over all REDOR evolution times. In the minimization of χ_ν^2, the $^{13}C-^{15}N$ dipolar coupling, b_{CN}, and the amplitude scaling factor λ were varied freely. The uncertainties are reported at 95% confidence limits. The values of b_{CN} and λ were then used in the DANTE−REDOR analysis. In calculation of r_{CN}, each value of b_{CN} was reduced by 5% to account for thermal motion at 298 K.[25,26] Similarly, for determining α and β, which define the orientation of the $^{13}C-^{15}N$ dipolar vector in the CSA PAS frame, the analytical equations[12] for REDOR sideband dephasing were used to minimize

$$\chi_\nu^2 \propto \sqrt{\sum_j \left(\left(\left(\frac{\Delta S}{S_0}\right)_{i,\,\mathrm{exp}} - \left(\frac{\Delta S}{S_0}\right)_{i,\,\mathrm{sim}}\right)/l\right)^2}$$

where the sum is taken over all REDOR sidebands j for a single REDOR evolution time, and l is the total number of sidebands used (including the center band).

In determining both distances from $^{13}C'$ to the imidazole ^{15}Ns and the $^{13}C'-^{15}N_\epsilon$ CSA/dipolar orientation on the 1:9 dilution sample, it was necessary to account for intermolecular $^{13}C-^{15}N$ dipolar couplings from next-nearest neighbors. For the $C'-N_\delta$ spin pair, the two closest intermolecular distances are 3.49 and 4.65 Å and for $C'-N_\epsilon$ spin pair, the two closest intermolecular distances are 3.67 and 4.85 Å. No correction was necessary for the $^{13}C'-^{15}N_\delta$ CSA/dipolar orientation measurements as these experiments were performed on a 1:19 sample. For the r_{CN} distance measurements, $^{13}C\{^{15}N\}$REDOR curves for the two CNN spin-systems and the CNNN spin-system were calculated using atom positions from the X-ray structure and added to the calculated isolated spin pair $^{13}C\{^{15}N\}$REDOR dephasing curve. For the $^{13}C'-^{15}N_\epsilon$ sideband REDOR dephasing on the 1:9 diluted sample, corresponding S and S_0 spectra for the intermolecular dephasing were calculated using the SIMPSON simulation package.[27] The contribution from intermolecular couplings has been subtracted for the $^{13}C'-^{15}N_\epsilon$ $^{13}C\{^{15}N\}$DANTE−REDOR data shown below. The relative weighting for the calculated REDOR curves are 0.81, 0.09, and 0.01 for the two-spin, three-spin, and four-spin systems, respectively.

Conformational Search. The backbone $^{13}C'-^{15}N'$ distance and angles determined from the DANTE−REDOR experiment were used to orient the principal axis system (PAS) of the C′ CSA tensor in the molecular frame and were used in all following calculations. Conformational searches (MacroModel, Schrodinger, LLC.) were performed to determine all possible structures consistent with the NMR data.

Macromodel was used to rotate the ψ, χ_1, and χ_2 torsional angles of the L-histidine·HCl·H_2O crystal structure. Only those structures meeting the distance and angle restraints were kept. No energy minimization was performed during any steps. All bond angles and distances were kept from the crystal structure. The carboxyl group atoms and the C′ CSA PAS were not allowed to move during the conformational search and therefore are identical for all structures.

Results and Discussion

Polycrystalline U-[$^{13}C_6$,$^{15}N_3$]-L-histidine·HCl·H_2O provides a stringent test of the DANTE−REDOR experiment as it contains features salient to larger systems: $^1J_{CC}$ and $^1J_{CN}$ couplings, multiple ^{13}C and ^{15}N resonances, carbons with large CSAs, a manifold of rotational resonance conditions, and a nontrivial side-chain conformation. To ensure constancy, an X-ray structure was determined for a crystal representative of the polycrystalline sample, which matched the literature structure.[28] We verified that all subsequent polycrystalline samples matched this structure using X-ray powder diffraction (see Figure S1).

To determine the imidazole side-chain conformation, we chose to measure the distances and orientations of the two imidazole nitrogens (N_δ, N_ϵ) with respect to the backbone carboxyl carbon (C′). For a $^{13}C-^{15}N$ spin pair, the orientation of the C−N dipolar vector in the ^{13}C CSA frame can be specified by the azimuthal (α) and polar (β) angles, as shown in Figure 2. To relate the measured α and β to specific structural constraints, the magnitude and orientation of the principal components (δ_{11}, δ_{22}, δ_{33}) of the $^{13}C'$ CSA frame relative to the local molecular geometry must be known a priori. The magnitude of the $^{13}C'$ CSA principal tensor components can be readily ascertained[21] from the ^{13}C CP/MAS spectrum to be δ_{11}

(21) Herzfeld, J.; Berger, A. E. *J. Chem. Phys.* **1980**, *73*, 6021−6030.
(22) Eichele, K.; Wasylishen, R. E. Dalhousie University and Universität Tübingen: 2006.
(23) Hohwy, M.; Rienstra, C. M.; Jaroniec, C. P.; Griffin, R. G. *J. Chem. Phys.* **1999**, *110*, 7983−7992.
(24) Raleigh, D. P.; Levitt, M. H.; Griffin, R. G. *Chem. Phys. Lett.* **1988**, *146*, 71−76.
(25) Ishii, Y.; Terao, T.; Hayashi, S. *J. Chem. Phys.* **1997**, *107*, 2760−2774.
(26) McDowell, L. M.; Klug, C. A.; Beusen, D. D.; Schaefer, J. *Biochemistry* **1996**, *35*, 5395−5403.
(27) Bak, M.; Rasmussen, J. T.; Nielsen, N. C. *J. Magn. Reson.* **2000**, *147*, 296−330.
(28) Oda, K.; Koyama, H. *Acta Cryst. B* **1972**, *B28*, 639−642.

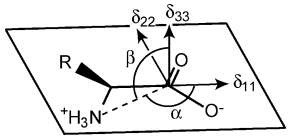

Figure 2. Azimuthal (α) and polar (*β*) angles defining the orientation of the $^{13}C-^{15}N$ dipolar vector in the principal axis system of the backbone ^{13}C CSA tensor. δ_{11} and δ_{22} lie in the OCO plane and δ_{33} is perpendicular to this plane.

Table 1. Summary of Distance and Orientation Measurements[a]

pair	exptl dist	X–ray dist	exptl α,*β*	X–ray α,*β*
C′−N′	2.5 ± 0.1 Å	2.48 Å	150 ± 7°, 85 ± 15°	
C′−Nϵ	4.1 ± 0.3 Å	4.37 Å	106 ± 90°, 158 ± 15°	93°, 163°
C′−Nδ	4.2 ± 0.3 Å	4.29 Å	170 ± 45°, 147 ± 9°	155°, 147°

[a] The X-ray α,*β* values were calculated by orienting the C′ CSA tensor in the X-ray structure with the NMR measured α, *β* values for C′−N′ (Figure 3).

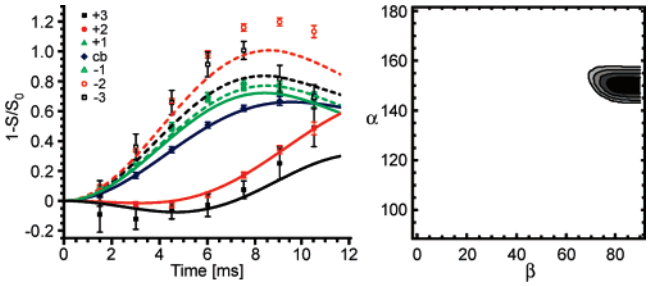

Figure 3. $^{13}C\{^{15}N\}$DANTE−REDOR dephasing (left) for the isotropic resonance (cb) and spinning sidebands of the carboxyl carbon ($^{13}C'$) dephased by the backbone nitrogen ($^{15}N'$) of U-[$^{13}C_6$,$^{15}N_3$]-L-histidine·HCl·H_2O. The best-fit REDOR curves are shown as lines. Labeled histidine was diluted to 10% in natural abundance histidine. The χ^2 surface is shown on the right for azimuthal (α) and polar (*β*) angles of the CSA−dipole orientation, with the best fit at r_{CN} = 2.5 Å, α = 150°, *β* = 85°.

= 65.2, δ_{22} = −6.4 and δ_{33} = −58.8 ppm, which compare well to previously published values for this crystalline polymorph.[29,30] The backbone $^{13}C'-^{15}N'$ distance was measured by fitting the sum of the REDOR dephasing over the +3 to −3 sidebands to the analytical[12] REDOR expression. This r_{CN} was found to agree well with the X-ray determined distance (Table 1). In principle, this information can be extracted from a single REDOR evolution time but, as shown in the DANTE−REDOR curve in Figure 3, seven REDOR points were used. To determine the CSA−dipole orientation of the backbone $^{13}C'-^{15}N'$ spin pair the observed DANTE−REDOR sideband dephasing for a single REDOR evolution time of 6.016 ms was fit using previously derived analytical expressions[12] (Figure 3 and Table 1). Figure 3-right shows the values of α and *β* angles that best fit the $^{13}C\{^{15}N\}$DANTE−REDOR data within experimental error. Similar results are obtained if only the ±1 sidebands are used. The C′ and N′ X-ray atom positions were then used to orient the $^{13}C'$ CSA tensor in the molecular frame. This measurement places the $^{13}C'$ δ_{11} nearly bisecting the OCO angle and δ_{33} approximately normal to the OCO plane. This is very similar to the $^{13}C'$ CSA tensor orientation determined for glycine[31] and alanine.[12,32] For a protein sample, canonical

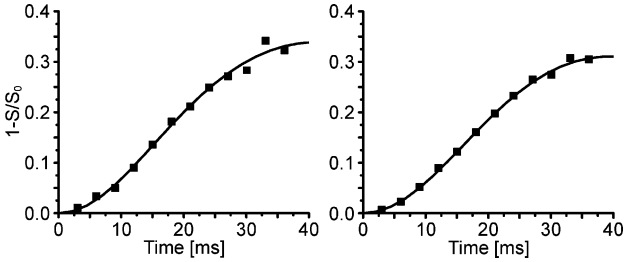

Figure 4. $^{13}C\{^{15}N\}$DANTE−REDOR curves for $^{13}C'-^{15}N_\delta$ (left) and $^{13}C'-^{15}N_\epsilon$ (right) in U-[$^{13}C_6$,$^{15}N_3$]-L-histidine·HCl·H_2O diluted 1:9 with natural abundance histidine. The solid lines are calculated REDOR dephasing curves with $^{13}C-^{15}N$ distances of 4.2 and 4.1 Å for N_δ and N_ϵ, respectively. These curves also include contributions from intermolecular dipolar couplings to next-nearest neighbors.

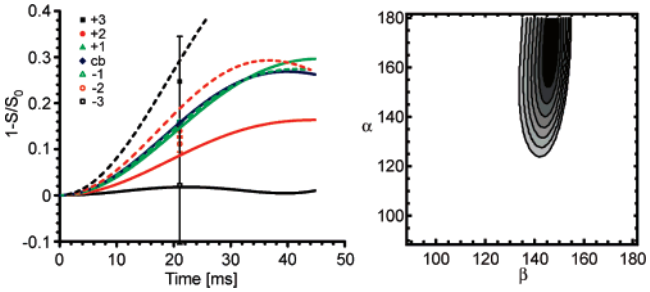

Figure 5. $^{13}C\{^{15}N\}$DANTE−REDOR dephasing for isotropic resonance and spinning sidebands of backbone $^{13}C'$ dephased by imidazole side chain $^{15}N_\delta$ of U-[$^{13}C_6$,$^{15}N_3$]-L-histidine·HCl·H_2O diluted 1:19 with natural abundance histidine (left) and the χ^2 surface of azimuthal (α) and polar (*β*) angles for the internuclear $^{13}C-^{15}N$ dipolar vector in the PAS of the C′ carbon CSA tensor (right). Lines in the left figure show the best fit at r_{CN} = 4.2 Å, α = 170°, *β* = 147°.

values[33−36] for α and *β* for the backbone carbonyl carbon can be used once the backbone secondary structure is gleaned from the $^{13}C'$ isotropic chemical shift.[37]

The NMR-determined distances and orientations for $C'-N_\epsilon$ and $C'-N_\delta$ in histidine, each derived from separate DANTE-selected REDOR experiments, are shown in Figures 4 to 6 and summarized in Table 1. The NMR-determined distances (Figure 4) match well to the X-ray distances. For the $C'-N_\delta$ pair, the χ^2 surface shows a well-defined global minimum at α = 170°, *β* = 147° (Figure 5), which agrees with the orientation expected from the crystal structure (α = 155°, *β* = 147°). For the $C'-N_\epsilon$ spin pair, the expected polar angle (*β*) from the crystal structure (163°) matches well with that calculated from the REDOR dephasing (158°). Since *β* is close to 180°, the sideband dephasing rates are nearly independent of α, as manifested in the χ^2 fit (Figure 6) and the relatively high error in α. In both cases, a single REDOR evolution time was sufficient to determine α and *β*. This proved to be an effective strategy with the lower signal-to-noise found in the 5% dilution sample.

We then constructed families of structures consistent with the three sets of experimentally derived distance and orientation

(29) Ye, C.; Fu, R.; Hu, J.; Hou, L.; Ding, S. *Magn. Reson. Chem.* **1993**, *31*, 699−704.
(30) Strohmeier, M.; Stueber, D.; Grant, D. M. *J. Phys. Chem. A* **2003**, *107*, 7629−7642.
(31) Haberkorn, R. A.; Stark, R. E.; van Willigen, H.; Griffin, R. G. *J. Am. Chem. Soc.* **1981**, *103*, 2534−2539.
(32) Naito, A.; Ganapathy, S.; Akasaka, K.; McDowell, C. A. *J. Chem. Phys.* **1981**, *74*, 3190−3197.
(33) Hartzell, C. J.; Pratum, T. K.; Drobny, G. P. *J. Chem. Phys.* **1987**, *87*, 4324−4331.
(34) Oas, T. G.; Hartzell, C. J.; McMahon, T. J.; Drobny, G. P.; Dahlquist, F. W. *J. Am. Chem. Soc.* **1987**, *109*, 5956−5962.
(35) Teng, Q.; Iqbal, M.; Cross, T. A. *J. Am. Chem. Soc.* **1992**, *114*, 5312−5321.
(36) Tan, W. M.; Gu, Z.; Zeri, A. C.; Opella, S. J. *J. Biomol. NMR* **1999**, *13*, 337−342.
(37) Zhang, H. Y.; Neal, S.; Wishart, D. S. *J. Biomol. NMR* **2003**, *25*, 173−195.

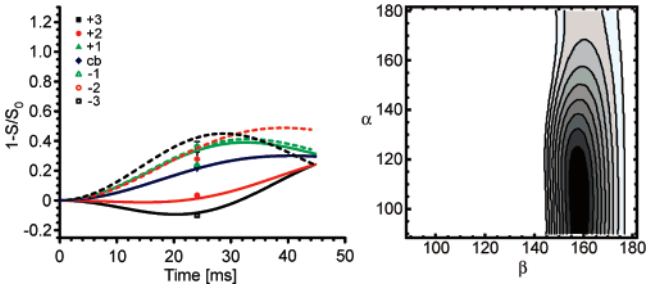

Figure 6. $^{13}C\{^{15}N\}$DANTE−REDOR dephasing for isotropic resonance and spinning sidebands of backbone C′ dephased by imidazole side chain $^{15}N_\epsilon$ of U-[$^{13}C_6$,$^{15}N_3$]-L-histidine·HCl·H_2O diluted 1:9 with natural abundance histidine (left) and the χ^2 surface for azimuthal (α) and polar (β) angles of the internuclear $^{13}C-^{15}N$ dipolar vector in the PAS frame of the C′ carbon CSA tensor (right). Lines in left figure show the best fit at r_{CN} = 4.1 Å, α = 106°, β = 158°. As β is close to the pole, α is poorly defined. Fits account for contributions from intermolecular ^{15}N dephasing from the two next-nearest neighbors.

constraints. These structures were generated by performing a conformational search of the φ (C′−C_α), χ_1 (C_α−C_β) and χ_2 (C_β−C_γ) dihedral angles. The results are shown in Figure 7. Points in white near the C′ (carboxyl) carbon indicate the principal axes of that carbon's CSA tensor frame of reference, with the crystal structure overlaid in red. Carboxyl group atoms and the C′ PAS were not allowed to move during the conformational search and therefore are identical for all structures. Conformations consistent with only the C′−N_δ distance are shown in Figure 7A and conformations consistent with both C′−N_δ and C′−N_ϵ distances are shown in Figure 7B. A single backbone ^{13}C−side chain ^{15}N distance is not sufficient to accurately constrain the imidazole side-chain orientation, as shown by the large rmsd (5.1 Å for the imidazole ring atoms) and the structures in Figure 7A. Two backbone ^{13}C and ring ^{15}N distances spatially confine the histidine side chain to a smaller region, but still do not correctly orient the imidazole ring (Figure 7B). Further families of structures and calculated rmsd using restricted subsets of the values in Table 1 are shown in the Supporting Information and demonstrate that using a single distance and orientation between backbone ^{13}C and ring ^{15}N as restraints results in families of structures that have at least two subsets of ring orientations. Figure 7D displays the resulting conformations consistent with all the constraints in Table 1, which gives the correct ring orientation and a 0.6 Å rmsd. Using no backbone-to-side-chain distance restraints and only C′−N_δ and C′−N_ϵ orientations results in a family of structures (Figure 7C) that almost matches the X-ray structure as well as the using of all the restraints listed in Table 1. By reproducing the X-ray structure, these results clearly show that a combination of distances and orientations resulting from the DANTE−REDOR experiment is sufficient to constrain global structure.

The restricted subset of backbone C′−N_δ and C′−N_ϵ orientation restraints (Figure 7C) perform almost as well as all the restraints listed in Table 1 (Figure 7D). Therefore, it is not always necessary to accurately determine both internuclear distances and orientations from the REDOR sideband dephasing.[5] In the case of the polycrystalline single amino acid histidine above, N_δ DANTE−REDOR data was collected using a 5% diluted sample; however, similar results were obtained for 10% dilution (data not shown). This indicates that even when ∼10% of $^{13}C'$ are coupled to interfering ^{15}N's ∼5 Å away, as may be

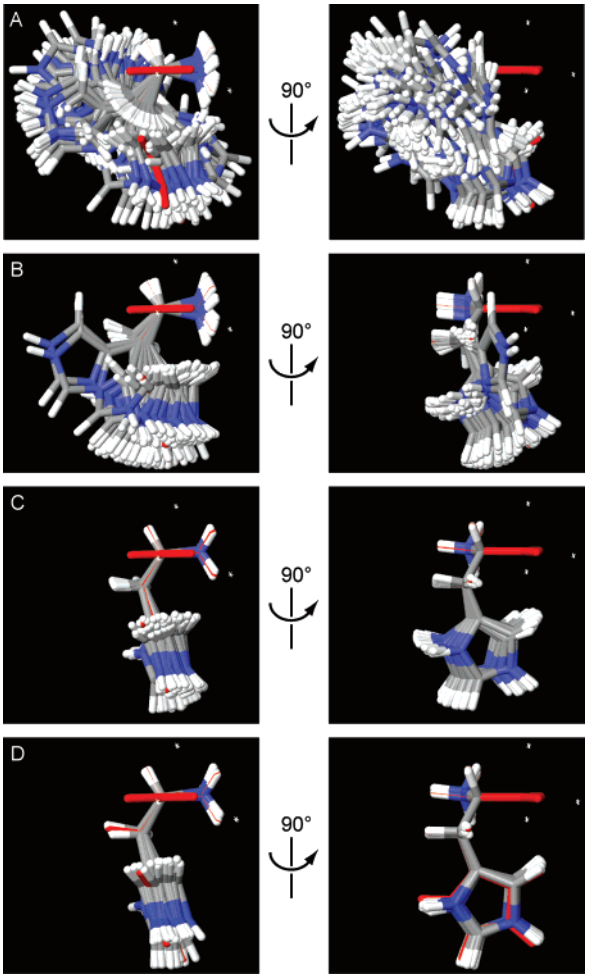

Figure 7. Structures consistent with (A) C′−N_δ distance, (B) C′−N_δ and C′−N_ϵ distances, (C) C′−N_δ and C′−N_ϵ orientations, and (D) all distances and orientations shown in Table 1. The rmsd for imidazole ring carbon and nitrogen atoms are 5.1, 2.4, 0.8, and 0.6 Å for A, B, C, and D, respectively. Backbone C′−N′ distance and orientation restraints were included in all conformational searches. Carboxyl group atoms and the C′ CSA tensor principal axes system were fixed during the conformational searches and are therefore identical in all structures. The X-ray structure is shown in red. White dots indicate principal axes of $^{13}C'$ CSA tensor.

found in a uniformly or selectively[4,38−41] $^{13}C/^{15}N$ enriched protein sample, the orientation can still be extracted from DANTE−REDOR sideband dephasing rates.

In the present case, accurately determining the orientation of the imidazole side chain does require knowledge of the backbone conformation. This can be obtained either from measuring the $^{13}CO-^{15}N'$ r_{CN}, α and β, as above, or from relating the ^{13}CO chemical shift to protein secondary structure.[37] Furthermore, we have found that for histidine two sets of r_{CN} distance and orientation (α and β) constraints, between side-chain ^{15}Ns and the backbone $^{13}C'$, are necessary to converge on the correct side-chain conformation. This requires three separate $^{13}C\{^{15}N\}$-DANTE−REDOR NMR measurements, which can all be performed on a single uniformly (^{13}C,^{15}N)-enriched sample. Interestingly, even though the uncertainty for α is quite large

(38) Hong, M. *J. Magn. Reson.* **1999**, *139*, 389−401.
(39) van Gammeren, A. J.; Hulsbergen, F. B.; Hollander, J. G.; de Groot, H. J. M. *J. Biomol. NMR* **2004**, *30*, 267−274.
(40) Hong, M.; Jakes, K. *J. Biomol. NMR* **1999**, *14*, 71−74.
(41) LeMaster, D. M.; Kushlan, D. M. *J. Am. Chem. Soc.* **1996**, *118*, 9255−9264.

for both backbone−side-chain measurements, the utilization of multiple restraints in the conformational searches resulted in a very well determined system even when the distance restraints were not used (Figure 7C). Distance and orientation constraints between ring ^{13}C to backbone ^{15}N spin-pairs can also be used to generate similar families of structures. However, under the conditions used here, the short ^{13}C T_2 relaxation led to low signal-to-noise.

Reintroduction of the ~2 kHz dipolar coupling between the directly bonded $^{13}CO-^{13}C_\alpha$ pair at the $n = 1$, 2, and 3 rotational resonance (R^2) conditions alters both S and S_0 DANTE−REDOR spectra (data not shown) thus invalidating application of the general equations[12] derived for extracting orientations from REDOR sideband dephasing. As well, inadequate refocusing of the $^1J_{CC}$ coupling between the directly bonded C′ and C_α will result in evolution of antiphase coherences resulting in a distorted line shape.[13] In typical protein samples, a spinning speed of 7.5 kHz on a 600 MHz NMR instrument puts the C_α carbon aliphatic region between the $n = 2$ and $n = 3$ R^2 conditions for the backbone carbonyl carbons.[42] At this spinning speed enough sidebands are present to accurately determine the side-chain orientation. Therefore, choosing a spinning speed such that the directly bonded C_α is outside of the selective DANTE pulse envelope is adequate for the DANTE−REDOR experiment. As has been demonstrated previously,[12] the relative dipolar−CSA orientation is encoded even when only a single set of sidebands is present, suggesting that orientations can still be measured when accurate peak intensities are unavailable owing to overlap with background resonances. However, the use of more sidebands does reduce the error on α and β. Although this implies that faster spinning speeds can be used, where only a single sideband is present, the sideband signal-to-noise at these elevated spinning speeds may be so weak that an extraordinary amount of spectrometer time would be required to collect the DANTE−REDOR spectra.

Conclusion

Structural determination of biological solids by solid-state NMR presents numerous challenges. Internuclear $^{13}C-^{15}N$ distances greater than 4 Å require long REDOR dephasing times, often exceeding 30 milliseconds. The slower spinning speeds necessary to produce a spinning sideband manifold, spin−spin relaxation, J couplings in a tightly coupled spin network and insufficient ^1H decoupling can impose harsh limits on the overall dephasing time that yields adequate signal. ^{15}N relaxation during the DANTE selection pulse train can lead to imperfect ^{13}C and ^{15}N inversion, resulting in only partial reintroduction of the dipolar coupling of interest and thus amplitude scaling of the REDOR curve. Uniform labeling gives rise to a web of rotational resonance conditions, harbingers of unwanted coherence transfer pathways. The histidine system investigated here is a good microcosm for all these issues, and we have shown that they can be addressed in reasonable fashion within the DANTE−REDOR experiment to arrive at an accurate overall structure. Refocusing both the center band, as first demonstrated with the FS-REDOR sequence,[3] and sidebands allows one to simultaneously extract both molecular orientation information and interatomic distances of chemical-shift resolved resonances. An advantage of the DANTE−REDOR experiment is that the analytic expressions[12] describing the distance and orientation dependence of the REDOR dephasing are directly applicable in this hybrid experiment to multiply labeled systems.

Extending the DANTE−REDOR experiment to larger peptide and protein systems will bring a mix of new challenges and some relief. As the number of spins increases, the rotational resonance map will become more congested. It may appear that this will eventually preclude a spinning speed with a sufficient number of spinning sidebands to yield useful orientation constraints, but this need not be so. Using labeling schemes with less than uniform labeling and performing the experiment at higher magnetic field strengths are two possible ways out of this predicament. The performance of the experiment is expected to improve at higher magnetic field strengths (14.1 T and above) as increased spectral dispersion will allow for selection of more spin pairs and faster spinning will decrease the time required for pair selection. The range of conformational possibilities may also grow rapidly. Most likely, residue side chains in longer peptide chains will exhibit fewer degrees of conformational freedom due to increased steric hindrance, thus leading to a smaller set of conformational possibilities. In practical terms, this may actually require fewer experimental restraints, and thus fewer experiments, to arrive at the correct conformation. By adding in energy constraints at the molecular modeling stage, convergence toward a global structure may in fact be more rapid than for the case presented here.

A distribution of conformations in heterogeneous systems will convolute the data. Because of the $1/r^3$ dependence of the dipolar coupling, conformations with shorter and longer internuclear distances will disproportionately weight a REDOR data set. Equivalently, different orientations will affect the dephasing rates of the individual sidebands. It should be possible to extract meaningful information about conformational heterogeneity by incorporating a distribution of structures in the numerical simulations.[43] Finally, even though we state that the individual resonances must be shift-resolved for the DANTE−REDOR experiment to function, this may not be a strict criterion. Because of the local nature of the REDOR experiment, only spin pairs less than 6 Å apart will dephase one another. Thus, even if spectral resonances overlap, the signal from the distant ^{13}C will only result in amplitude scaling of the REDOR curve and not affect the relative sideband dephasing rates.

We have described a new NMR experiment that can be used to elucidate global secondary structure in the solid state by combining distance and orientation constraints determined under moderate experimental conditions. This experiment builds on the observation that the dephasing of individual sidebands in a REDOR experiment encodes orientation information,[11,12] which we have extended to multiply labeled systems. The $^{13}C\{^{15}N\}$-DANTE−REDOR experiment enables spatial location of a nitrogen-containing side chain and it can be used to measure the ψ Ramachandran torsion angle in any residue. Although the selection of each specific pair of ^{13}C and ^{15}N resonances requires a separate experiment, the pulse sequence has the potential to triple the information content derived from any heteronuclear spin pair in a uniformly labeled solid sample. We

(42) Igumenova, T. I.; McDermott, A. E. *J. Magn. Reson.* **2003**, *164*, 270−285.

(43) Mehta, M. A.; Gregory, D. M.; Kiihne, S.; Mitchell, D. J.; Hatcher, M. E.; Shiels, J. C.; Drobny, G. P. *Solid State Nucl. Magn. Reson.* **1996**, *7*, 211−228.

expect the wealth of new structural constraints afforded by this experiment to be especially useful toward the ends of peptides where there is normally a paucity of $^{13}C-^{13}C$ and $^{13}C-^{15}N$ distances available to constrain the geometry. As long as the NMR resonances are resolved, the DANTE−REDOR experiment can be applied to systems with structural heterogeneity or in cases with large heterogeneous backgrounds, such as membranes and solid supports, and it can be used to measure CSA tensor orientations in polycrystalline solids, which is otherwise hard to do.

Acknowledgment. We thank the referees for insightful comments that helped strengthen the manuscript. L.B.A. and M.A.M. thank William Mohler (Oberlin College), Lon Buck, and Gary Drobny (University of Washington) for their help in the construction of an MAS controller; Manasi Bhate for growing the histidine crystals; Matthias Zeller and Allen Hunter (Youngstown State University) for determination of the histidine crystal structure. A.K.M. thanks David Lynn (Emory University) for encouragement and support and Jim Snyder for advice on conformational searches. Work at Oberlin College was supported by NSF-CAREER Grant CHE-0449629 and MRI Grant CHE-0079470 toward acquisition of a 600 MHz NMR spectrometer.

Supporting Information Available: NMR assignment data, X-ray data, and conformational searches. This material is available free of charge via the Internet at http://pubs.acs.org.

JA074789Q